

# ECG CLASSIFICATION COMPARISON BETWEEN MF-DFA AND MF-DXA

JIAN WANG

*School of Mathematics and Statistics  
Nanjing University of Information Science and Technology  
Nanjing 210044, P. R. China*

WEI SHAO

*School of Economics  
Nanjing University of Finance and Economics  
Nanjing 210023, P. R. China*

JUNSEOK KIM\*

*Department of Mathematics, Korea University  
Seoul 02841, Republic of Korea  
cfdkim@korea.ac.kr*

Received May 12, 2020

Accepted September 2, 2020

Published March 10, 2021

## Abstract

In this paper, automatic electrocardiogram (ECG) recognition and classification algorithms based on multifractal detrended fluctuation analysis (MF-DFA) and multifractal detrended cross-correlation analysis (MF-DXA) were studied. As human heart is a complex, nonlinear, chaotic system, using multifractal analysis to analyze chaotic systems is also a trend. We performed a comparison study of the multifractal nature of the healthy subjects and that of the cardiac dysfunctions ones. To analyze multifractal property quantitatively, the ranges of the Hurst exponent ( $\Delta h$ ) are computed by MF-DFA and MF-DXA. We found that for MF-DFA, the area of Hurst exponents for atrial premature beat (APB) people was narrower than normal sinus rhythm (NSR) subjects, and for MF-DXA, the difference of  $\Delta h$  ( $\Delta(\Delta h)$ ) of NSR and APB subjects was larger than that of MF-DFA. We then regarded the Hurst exponents

---

\*Corresponding author.

( $h$ ) as the input vectors and took them into support vector machine (SVM) for classification. The results showed that  $h$  obtained from MF-DXA led to a higher classification accuracy than that of MF-DFA. This is related to the widening of the difference in the values of Hurst exponents in MF-DFA and MF-DXA. The proposed MF-DFA-SVM and MF-DXA-SVM systems achieved classification accuracy of  $86.54\% \pm 0.068\%$  and  $98.63\% \pm 0.0644\%$ , achieved classification sensitivity of  $75.03\% \pm 0.1323\%$  and  $90.77\% \pm 0.1309\%$ , achieved classification specificity of  $86.66\% \pm 0.1131\%$  and  $96.47\% \pm 0.0891\%$ , respectively. In general, the Hurst exponents obtained from MF-DXA played an important role in classifying ECG of the healthy and that of the cardiac dysfunctions subjects. Moreover, MF-DXA was more accurate than MF-DFA in the classification of ECG studied in this paper. The research in automatic medical diagnosis and early warning of major diseases has very important practical value.

*Keywords:* ECG; MF-DFA; MF-DXA; Classification; Hurst Exponent.

## 1. INTRODUCTION

The recognition, denoising and classification of electrocardiogram (ECG) signal is one of the research hotspots in the field of signal processing.<sup>1-3</sup> It is an urgent demand to find a non-invasive and relatively accurate method to diagnose and predict heart diseases, and it is also a task to be solved urgently in the field of biomedical and electrical science. At present, the diagnosis of clinical heart diseases depends on the diagnosis of doctors or adopts the machine to conduct linear analysis on the collected ECG signals.

With the further study of the heart system, researchers found that the heart system is a typical nonlinear system. Therefore, more and more researchers try to use the nonlinear analysis method to study the characteristics of ECG signal in order to realize the early accurate diagnosis of heart disease. In recent years, multifractal analysis has become an effective tool for the analysis of nonlinear systems, and has made rapid progress in various fields.<sup>4-11</sup> As one of multifractal analysis, multifractal detrended fluctuation analysis (MF-DFA) has been applied in the biosignal classification field such as DNA sequences,<sup>12,13</sup> electroencephalogram (EEG) signals,<sup>14,15</sup> MRIs,<sup>16,17</sup> ECG signals,<sup>18-20</sup> etc.

Various human heartbeat classification methods have been studied in the recent years. Zhang<sup>21</sup> presented a disease-specific feature selection algorithm which consists of a one-versus-one (OvO) features ranking stage and a feature search stage using support vector machine (SVM); and the proposed feature selection method achieved 86.66% classification accuracy. A model for ECG automatic classification based on the combination of multiple SVMs was

presented in Ref. 22. Their ensemble SVM acquired satisfactory performance with accuracy of 94.5%. Yildirim<sup>23</sup> employed a wavelet sequence based a long-short term memory (LSTM) network model for ECG signal classification with high classification performances of 99.39% with deep bidirectional LSTM network-based wavelet sequence (DBLSTM-WS) and 99.25% with deep unidirectional LSTM network-based wavelet sequence (DULSTM-WS). In Ref. 24, the authors applied the permutation entropy and the conditional entropy of ordinal patterns to ECG signal analysis, and classification rate of 93.62% was achieved. Rajesh *et al.*<sup>25</sup> classified ECG signals for the MIT-BIH database by using nonlinear decomposition methods and SVM, and the method acquired 99.20% accuracy, 98.01% sensitivity and 99.49% specificity.

Because the MF-DFA can easily obtain scale index and multifractal spectrum for non-stationary time series, and it can effectively analyze the multifractal characteristics of time series, MF-DFA is widely used in the analysis of ECG signals. Therefore, in this study, we first apply MF-DFA for ECG signals, and compute the mean  $\Delta h$  for normal sinus rhythm (NSR) and atrial premature beat (APB) subjects. Then, we take Hurst exponents as the input vectors SVM for classification. In addition, we also apply the multifractal detrended cross-correlation analysis (MF-DXA) method to analyze the ECG signals. MF-DXA is used to quantitatively analyze the cross-correlations of multifractal characteristics for two time series, and is combined by the detrended cross-correlation analysis (DCCA) and MF-DFA. The MF-DXA based on multifractal theory can effectively remove the influence of local trend on the scale of time series, and can detect the

multifractal characteristics of time series under different time scales. It is an effective method to study the long-term power-law cross-correlation between non-stationary time series. In order to show whether MF-DXA is more accurate than MF-DFA in classifying adults' ECG signals, we randomly select an ECG signal from NSR subjects as a fixed time series in MF-DXA, so as to enlarge the difference between the Hurst exponents of NSR and APB subjects, then the classification accuracy can be improved due to the increase of input vector difference in the classification process.

The collection of ECG signals analyzed in this paper was obtained from the PhysioNet service (<http://www.physionet.org>) from MIT-BIH Arrhythmia database. The ECG signals were collected from 45 patients including 26 adult male and 19 adult female whose age ranges from 23 to 89. All ECG signals were recorded at a sampling frequency of 360 Hz and a gain of 200 [adu/mV]. Data are in mat format and these data can be downloaded from: <https://data.mendeley.com/datasets/7dybx7wyfn/3>.

The paper is organized as follows. We briefly introduce the methodology in Sec. 2 and SVM in Sec. 3. Section 4 deals with empirical experiments and classification. Section 5 provides a conclusion.

## 2. MF-DXA

The MF-DXA method can be generally described as follows:

- (I) Given two time series  $\{x_t^{(1)}, x_t^{(2)}, t = 1, 2, \dots, N\}$  of the same length  $N$ , calculate the cumulative deviation series

$$X^{(i)}(t) = \sum_{k=1}^t (x_k^{(i)} - \overline{x^{(i)}}), \quad (1)$$

where  $\overline{x^{(i)}} = \frac{1}{N} \sum_{t=1}^N x^{(i)}(t)$ ,  $t = 1, 2, \dots, N$  and  $i = 1, 2$ .

- (II) Divide two profiles  $X^{(1)}$  and  $X^{(2)}$  into  $N_s = \text{int}(\frac{N}{s})$  non-overlapping segments of equal length  $s$ . Because  $N$  is generally not a multiple of the window size  $s$ , a short part of the time series remains in most cases. To include this part of the series, we repeat the same process from the opposite end of each time series. Thus,  $2N_s$  segments are obtained together.

- (III) Then, we acquire the local detrending of the segments by a polynomial fitting

$$x_v^{(i)}(j) = a_1 j^k + a_2 j^{k-1} + \dots + a_k j + a_{k+1},$$

$$j = 1, 2, \dots, s; k = 1, 2, \dots, i = 1, 2. \quad (2)$$

- (IV) Afterwards, calculate the detrended covariance  $F^2(s, v)$ . When  $v = 1, 2, \dots, N_s$ ,

$$F^2(s, v) = \frac{1}{s} \sum_{j=1}^s \{ |X^{(1)}[(v-1)s+j] - x_v^{(1)}(j)| |X^{(2)}[(v-1)s+j] - x_v^{(2)}(j)| \}. \quad (3)$$

When  $v = N_s + 1, N_s + 2, \dots, 2N_s$ ,

$$F^2(s, v) = \frac{1}{s} \sum_{j=1}^s \{ |X^{(1)}[N - (v - N_s)s + j] - x_v^{(1)}(j)| |X^{(2)}[N - (v - N_s)s + j] - x_v^{(2)}(j)| \}. \quad (4)$$

- (V) Average the detrended covariances and derive the  $q$ th-order detrended fluctuation function as

$$F_q(s) = \left\{ \frac{1}{2N_s} \sum_{v=1}^{2N_s} [F^2(s, v)]^{\frac{q}{2}} \right\}^{\frac{1}{q}}. \quad (5)$$

When  $q = 0$ ,

$$F_0(s) = \exp \left( \frac{1}{2N_s} \sum_{v=1}^{2N_s} \ln[F^2(s, v)] \right). \quad (6)$$

If scaling behavior and long-range correlations exist, then a power-law correlation satisfies  $F_q(s) \propto s^{h(q)}$ .  $h_{xy}(q)$  stands for the generalized Hurst exponent versus  $q$ , the degree of multifractality can be measured by the range of  $h(q)$ , a higher  $\Delta h = h(q)_{\max} - h(q)_{\min}$  results in stronger multifractal property.

## 3. SUPPORT VECTOR MACHINE

The SVM is a machine learning technique which is based on statistical learning theory.<sup>26</sup> It is based on Vapnik-Chervonenkis (VC) theory and structural risk minimization principle. It seeks the best compromise between the complexity of the model and the learning ability according to the limited sample information, so as to obtain better generalization ability. When SVM algorithm is used for classification, the basic idea is to map the data of the

input space into a high-dimensional feature space through a nonlinear mapping  $\phi(\cdot)$ , and then make linear classification in the high-dimensional space.

In a binary classification system of SVM, we solve convex quadratic programming problem and maximize the objective function of the dual problem as

$$\max_{\alpha} \left[ \sum_{i=1}^n \alpha_i - \frac{1}{2} \sum_{i,j=1}^n \alpha_i \alpha_j y_i y_j \langle \phi(x_i), \phi(x_j) \rangle \right], \quad (7)$$

where  $0 \leq \alpha_i, i = 1, 2, \dots, n$ , and  $\sum_{i=1}^n \alpha_i y_i = 0$ .

The inner product of two vectors after an implicit mapping in the above function is called the kernel function. As the Gaussian kernel always give a good linear separation in higher dimension, therefore, we use the Gaussian kernel in this paper as follows:

$$k(x_i, x_j) = e^{-\frac{\|x_i - x_j\|^2}{2\sigma^2}}. \quad (8)$$

Thus, the binary classification problem can be solved by Eq. (9)

$$\max_{\alpha} \left[ \sum_{i=1}^n \alpha_i - \frac{1}{2} \sum_{i,j=1}^n \alpha_i \alpha_j y_i y_j k(x_i, x_j) \right]. \quad (9)$$

In this study, we define NSR as class -1 and APB as class 1, and the classifier equation is denoted as

$$y(x) = \text{sign} \left( \sum_{i=1}^n \alpha_i y_i k(x_i, x) + b \right), \quad (10)$$

where  $b$  is a bias.

#### 4. COMPUTATIONAL RESULTS

Now, we perform several computational experiments to demonstrate the robustness and efficiency of the proposed method. ECG signals from NSR and APB categories in MIT-BIH Arrhythmia database are selected for this study. Here, NSR category is composed of 283 NSR signals and APB is consisted of 66 APB signals. Each signal series is consisted of 3600 points. According to Refs. 27 and 28, the segment size is chosen from  $s_{\min} = 100$  to the maximum segment scale  $s_{\max} = N/10$ , for this case, select 11 segment values of equal spacing from the segment scale interval. The fractal-order  $q$  is chosen by  $-10, -6, -2, 2, 6, 10$ . Firstly, we select two pieces of ECG signals with complete ECG cycle. During the selection process, we ensure that the two ECG signals are taken from NSR and APB respectively, and are randomly selected, as shown in Fig. 1.

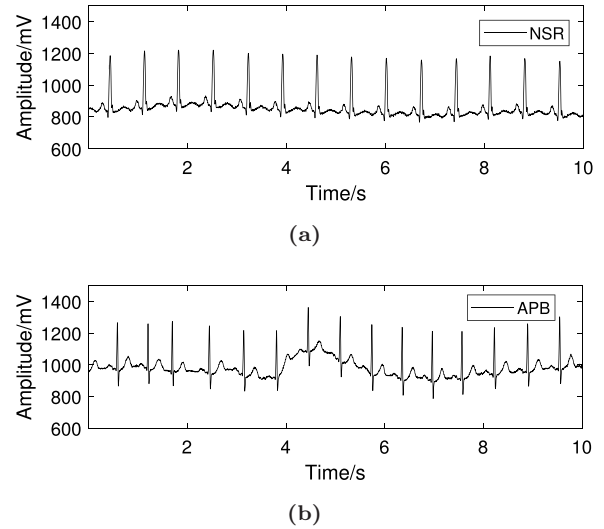


Fig. 1 ECG signal time series for (a) NSR and (b) APB.

Then, MF-DFA is applied to the two ECG time series to obtain the corresponding generalized Hurst exponents distribution, as shown in Fig. 2. From the multifractal method, we can know that the relationship between the generalized Hurst exponents  $h(q)$  and  $q$  can be used as the main basis to evaluate whether time series has multifractal. It can be seen from Fig. 2 that there is an obvious decreasing relationship between  $h(q)$  and  $q$  of these two ECG time series. Therefore, it can be concluded that the ECG signals of NSR and APB are multifractal. Besides, when  $q$  is between  $-5$  and  $5$ , the multifractal property of ECG signal is the most obvious, and while  $q < -5$  or  $q > 5$ , the change speed of generalized Hurst exponents obviously slows down.

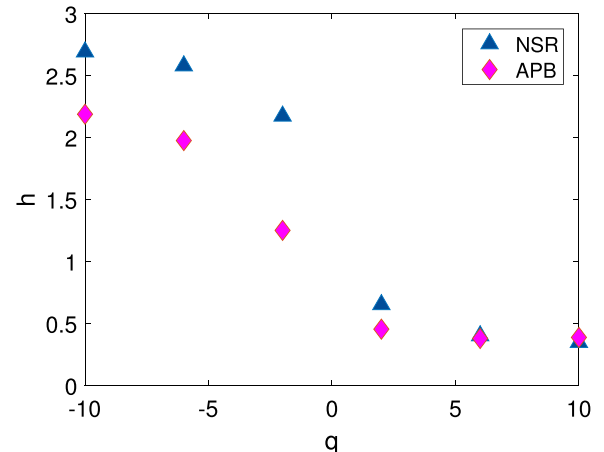
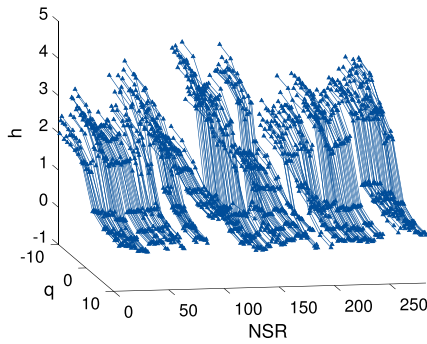
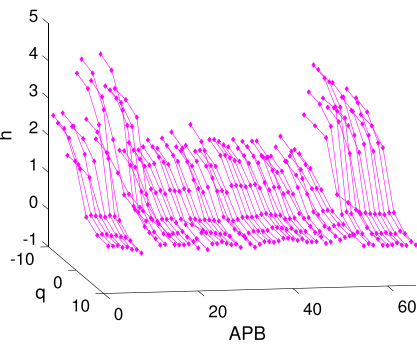


Fig. 2 Generalized Hurst exponents of randomly selected two NSR and APB signals.



(a)



(b)

**Fig. 3** Generalized Hurst exponents of (a) 283 NSR signals and (b) 66 APB signals using MF-DFA.

After reconfirming the multifractality of ECG signals, we use MF-DFA method to extract the variation of generalized Hurst exponents from 283 signals in NSR and 66 signals in APB, the corresponding generalized Hurst exponents curves are depicted in Fig. 3. As shown in the figure, the distribution of generalized Hurst exponents for NSR and APB

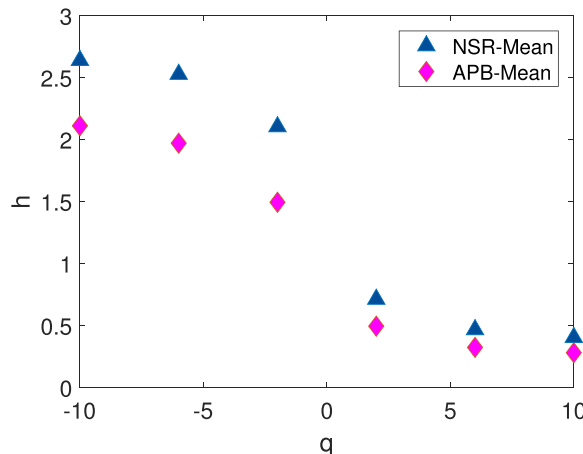


**Fig. 4** Generalized Hurst exponents of mean value of NSR signals and APB signals using MF-DFA.

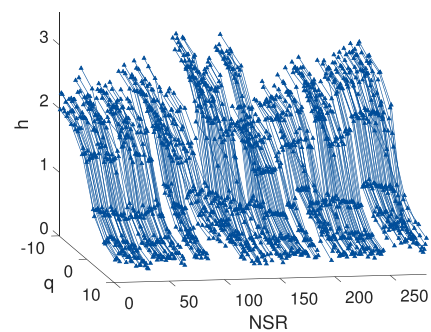
**Table 1** Statistics of Mean Values of Hurst Exponents.

| ECG         | $h_{\min}$ | $h_{\max}$ | $\Delta h$ | $\Delta(\Delta h)$ |
|-------------|------------|------------|------------|--------------------|
| NSR(MF-DFA) | 0.4033     | 2.6376     | 2.2343     |                    |
| ABP(MF-DFA) | 0.2801     | 2.1103     | 1.8302     | 0.4041             |
| NSR(MF-DXA) | 0.4798     | 2.2681     | 1.7883     |                    |
| ABP(MF-DXA) | 0.3872     | 1.5724     | 1.1852     | 0.6031             |

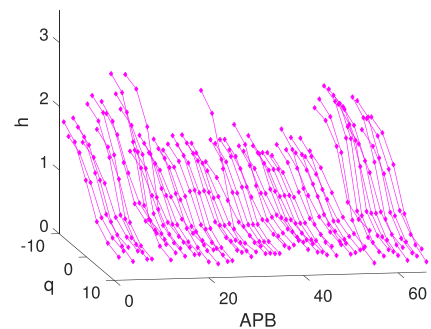
ECG signals are different. In order to show the difference more intuitively, we mean these Hurst exponents and plot them in Fig. 4. We extract the maximum value, the minimum value and the difference between two metrics, and list them in Table 1.

Since the  $\Delta h$  of NSR signal is larger than ABP signal, indicating the multifractal degree of NSR signal is stronger than that of ABP signal.

Afterwards, we conduct MF-DXA method for NSR and APB signals. We randomly select the an ECG signal from NSR subjects as a fixed time series of MF-DXA, we aim to enlarge the difference between the Hurst exponents of NSR and APB subjects, thereby the classification accuracy can be improved due to the increase of input vector difference in the classification process. As shown in



(a)



(b)

**Fig. 5** Generalized Hurst exponents of (a) 283 NSR signals and (b) 66 APB signals using MF-DXA.

Fig. 5, the distribution of generalized Hurst exponents calculated by MF-DXA for 283 NSR and 66 APB ECG signals show different and are also different from Fig. 3. When compared to Fig. 3, the difference between the values of the Hurst exponents of NSR and APB is expanding, the volatility of the Hurst exponents of the two categories are smaller than that of MF-DFA, and their characteristics tend to be more stable.

We compute the mean values of these Hurst exponents, and they are depicted in Fig. 6. Through the comparison of  $\Delta h$  of NSR and APB signals listed in Table 1, we observe that the NSR signal also has a greater multifractality since the  $\Delta h$  is higher than that of APB. In addition, we also note that for MF-DXA, the difference of  $\Delta h$  ( $\Delta(\Delta h)$ ) of NSR and APB subjects is larger than that of MF-DFA, implying the characteristics differences have been widened when MF-DXA is used, which may result in improving the classification accuracy of NSR and APB ECG signals.

To verify the classification efficiency of MF-DFA and MF-DXA, we regard the generalized Hurst exponents in Figs. 3 and 5 as the input training vectors, the classification process is conducted by SVM. For more detailed information, please refer to Ref. 26. The calculated generalized Hurst exponents of the healthy ECG signals are labeled by value  $-1$ , while Atrial Premature Beat signals are labeled by class 1. The leave-one-out cross-validation method<sup>29</sup> is considered in this study. We simulate the process 100 times and use evaluation indicator such as accuracy, sensitivity and specificity to measure the performance of the models. TruePositive, FalseNegative, TrueNegative and FalsePositive are usually

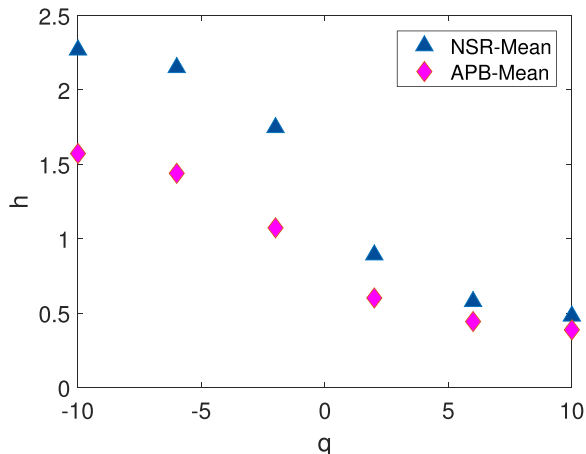


Fig. 6 Generalized Hurst exponents of mean value of NSR signals and APB signals using MF-DXA.

regarded as the variables taken for calculation for the following three metrics:

$$\text{Accuracy} = \frac{\text{TP} + \text{TN}}{\text{TP} + \text{FN} + \text{FP} + \text{TN}}, \quad (11)$$

$$\text{Sensitivity} = \frac{\text{TP}}{\text{TP} + \text{FN}}, \quad (12)$$

$$\text{Specificity} = \frac{\text{TN}}{\text{FP} + \text{TN}}, \quad (13)$$

where TP, FN, TN and FP are the abbreviations for TruePositive, FalseNegative, TrueNegative and FalsePositive, respectively.

The classification accuracy versus 100-times simulations for MF-DFA and MF-DXA are plotted in Fig. 7. We see that the classification accuracy curve of MF-DXA stay above much over that of MF-DFA, showing the classification effect of MF-DXA is much higher than MF-DFA. By calculation, the proposed MF-DFA-SVM system achieved classification accuracy of  $86.54\% \pm 0.068\%$ , while the MF-DXA-SVM system achieved classification accuracy of  $98.63\% \pm 0.0644\%$ .

In addition, we calculate the sensitivity for both methods, and the results versus simulation iterations are illustrated in Fig. 8. We see that MF-DXA achieved good performance by  $90.77\% \pm 0.1309\%$ , which is much larger than MF-DFA, the MF-DFA method achieved sensitivity by  $75.03\% \pm 0.1323\%$ .

At last, we calculate the specificity for both MF-DFA and MF-DXA methods, the results are depicted in Fig. 9. The MF-DFA and MF-DXA

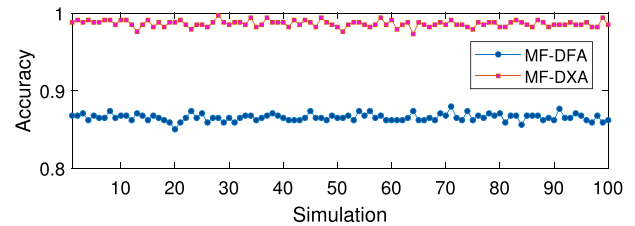


Fig. 7 Classification accuracy of MF-DFA and MF-DXA.

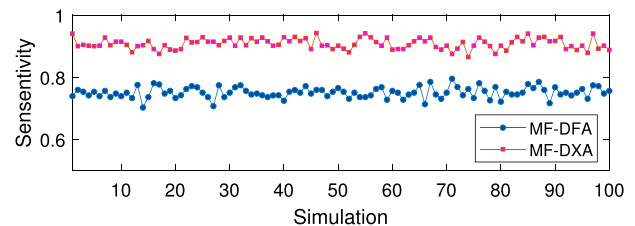


Fig. 8 Classification sensitivity of MF-DFA and MF-DXA.

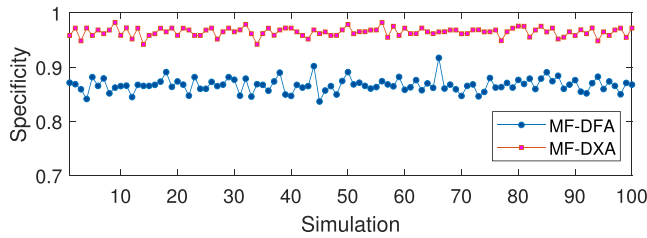


Fig. 9 Classification specificity of MF-DFA and MF-DXA.

Table 2 Statistics of Performance.

| Method             | MF-DFA-SVM          | MF-DXA-SVM          |
|--------------------|---------------------|---------------------|
| Accuracy           | 86.54% $\pm$ 0.068  | 98.63% $\pm$ 0.0644 |
| Sensentivity       | 75.03% $\pm$ 0.1323 | 90.77% $\pm$ 0.1309 |
| Specificity        | 86.66% $\pm$ 0.1131 | 96.47% $\pm$ 0.0891 |
| CPU time (seconds) | 1.23178             | 1.32105             |

achieved performance by 86.66%  $\pm$  0.1131% and 96.47%  $\pm$  0.0891%, respectively.

The performance of two proposed systems are summarized in Table 2. Besides, we also provide the CPU processing time of MF-DFA versus MF-DXA in the analysis of a single ECG record in Table 2. All the computations are processed by using Matlab R2018b on an Intel(R) Core(TM) i5-6200 CPU @ 2.30 GHz processor.

From Table 2, we observe that the classification performance of MF-DXA-SVM is much better than that of MF-DFA-SVM, while the CPU processing time of MF-DXA-SVM costs a little more than that of MF-DFA-SVM.

## 5. CONCLUSIONS

In this paper, we compared the performance of automatic ECG recognition and classification algorithms between MF-DFA and MF-DXA. Two categories of ECG signals such as normal sinus rhythm and atrial premature beat from MIT-BIH database are taken as research objects, and the multifractal characteristics of ECG signal time series are analyzed in detail from the perspectives of MF-DFA and MF-DXA. The results showed that the ranges of the Hurst exponent  $\Delta h$  for APB signals was narrower than NSR signals, indicating the multifractal characteristics of NSR signals was stronger than that of APB signals, and this phenomenon was also established by MF-DXA. We also found  $\Delta(\Delta h)$  of NSR and APB subjects of MF-DXA was larger than that of MF-DFA, implying the characteristics differences have been widened when MF-DXA was used. We then regarded the

Hurst exponents ( $h$ ) as the input vectors and took them into support vector machine for classification. The computational results demonstrated that all the classification accuracy, sensitivity and specificity of the proposed MF-DXA-SVM system are higher than that of the proposed MF-DFA-SVM. This solution is related to the widening of the difference in the values of Hurst exponents in MF-DFA and MF-DXA. Generally, the Hurst exponents obtained from MF-DXA played an important role in classifying ECG signals of NSR and APB. However, due to the amount of ECG signals of NSR and APB in MIT-BIH database is limited, we only analyzed the multifractal characteristics of the existing signals, which makes the analysis results may have some limitations. We will focus on each type of ECG signal and massive data in our future work, further analyze the multifractal characteristics of each disease, to provide a certain reliable basis for quantitative diagnosis and classification. In general, our study provided an effective analysis method for non-invasive heart disease diagnosis and classification of ECG signals.

## ACKNOWLEDGMENTS

The corresponding author (J. S. Kim) expresses thanks for the support from the BK21 FOUR program. The authors appreciate the reviewers for their constructive comments, which have improved the quality of this paper.

## REFERENCES

1. K. N. Rajesh and R. Dhuli, Classification of imbalanced ECG beats using re-sampling techniques and AdaBoost ensemble classifier, *Biomed. Signal Process. Control* **41** (2018) 242–254.
2. N. I. Hasan and A. Bhattacharjee, Deep learning approach to cardiovascular disease classification employing modified ECG signal from empirical mode decomposition, *Biomed. Signal Process. Control* **52** (2019) 128–140.
3. A. Zarei and B. M. Asl, Automatic classification of apnea and normal subjects using new features extracted from HRV and ECG-derived respiration signals, *Biomed. Signal Process. Control* **59** (2020) 101927.
4. J. W. Kantelhardt, S. A. Zschiegner and E. Koscielny-Bunde, Multifractal detrended fluctuation analysis of nonstationary time series, *Physica A* **316**(1) (2002) 87–114.
5. S. Lahmiri, Multifractal in volatility of family business stocks listed on Casablanca stock exchange, *Fractals* **25**(2) (2017) 1750014.

6. S. Lahmiri, Multifractals in western major stock markets historical volatilities in times of financial crisis, *Fractals* **25**(1) (2017) 1750010.
7. W. Shao and J. Wang, Does the “ice-breaking” of South and North Korea affect the South Korean financial market?, *Chaos Soliton. Fract.* **132** (2020) 109564.
8. S. Lahmiri and S. Bekiros, Chaos, randomness and multi-fractality in Bitcoin market, *Chaos Soliton. Fract.* **106** (2018) 28–34.
9. J. Wang, W. Shao and J. Kim, Cross-correlations between bacterial foodborne diseases and meteorological factors based on MF-DCCA: A case in South Korea, *Fractals* **28**(3) (2020) 2050046.
10. J. Wang, W. Shao and J. Kim. Automated classification for brain MRIs based on 2D MF-DFA method, *Fractals* (2020), <https://doi.org/10.1142/S0218348X20501091>.
11. S. Lahmiri, Multifractal analysis of Moroccan family business stock returns, *Phys. A* **486** (2017) 183–191.
12. C. Stan, M. T. Cristescu, B. I. Luiza and C. P. Cristescu, Investigation on series of length of coding and non-coding DNA sequences of bacteria using multifractal detrended cross-correlation analysis, *J. Theor. Biol.* **321** (2013) 54–62.
13. M. Pal, V. S. Kiran, P. M. Rao and P. Manimaran, Multifractal detrended cross-correlation analysis of genome sequences using chaos-game representation, *Phys. A* **456** (2016) 288–293.
14. S. Paul, A. Mazumder, P. Ghosh, D. N. Tibarewala and G. Vimalarani, EEG based emotion recognition system using MFDFA as feature extractor, in *2015 International Conference on Robotics, Automation, Control and Embedded Systems (RACE)* (IEEE, 2015), pp. 1–5.
15. S. Chatterjee, S. Pratiher and R. Bose, Multifractal detrended fluctuation analysis based novel feature extraction technique for automated detection of focal and non-focal electroencephalogram signals, *IET Sci. Meas. Technol.* **11**(8) (2017) 1014–1021.
16. S. Lahmiri and M. Boukadoum, Alzheimers disease detection in brain magnetic resonance images using multiscale fractal analysis, *ISRN Radiol.* (2013).
17. S. Lahmiri, Glioma detection based on multi-fractal features of segmented brain MRI by particle swarm optimization techniques, *Biomed. Signal Process. Control* **31** (2017) 148–155.
18. S. Dutta, Multifractal properties of ECG patterns of patients suffering from congestive heart failure, *J. Stat. Mech. Theory Exp.* **12** (2010) P12021.
19. J. Wang, X. Ning and Y. Chen, Multifractal analysis of electronic cardiogram taken from healthy and unhealthy adult subjects, *Phys. A* **323** (2003) 561–568.
20. H. M. Mercy Cleetus and D. Singh, Multifractal application on electrocardiogram, *J. Med. Eng. Technol.* **38**(1) (2014) 55–61.
21. Z. Zhang, J. Dong, X. Luo, K. S. Choi and X. Wu, Heartbeat classification using disease-specific feature selection, *Comput. Biol. Med.* **46** (2014) 79–89.
22. V. Mondéjar-Guerra, J. Novo, J. Rouco, M. G. Penedo and M. Ortega, Heartbeat classification fusing temporal and morphological information of ECGs via ensemble of classifiers, *Biomed. Signal Process. Control* **47** (2019) 41–48.
23. O. Yildirim, A novel wavelet sequence based on deep bidirectional LSTM network model for ECG signal classification, *Comput. Biol. Med.* **96** (2018) 189–202.
24. J. B. B. À Mougoufan, J. A. E. Fouda, M. Tchuenté and W. Koepf, Adaptive ECG beat classification by ordinal pattern based entropies, *Commun. Nonlinear Sci.* **84** (2020) 105156.
25. K. N. Rajesh and R. Dhuli, Classification of ECG heartbeats using nonlinear decomposition methods and support vector machine, *Comput. Biol. Med.* **87** (2017) 271–284.
26. V. Vapnik, *The Nature of Statistical Learning Theory* (Springer-Verlag, New York, 1995).
27. C. H. Shen, Y. Huang and Y. N. Yan, An analysis of multifractal characteristics of API time series in Nanjing, China, *Phys. A* **451** (2016) 171–179.
28. Q. Wang, Multifractal characterization of air polluted time series in China, *Phys. A* **514** (2019) 167–180.
29. Q. F. Gronau and E. J. Wagenmakers, Limitations of Bayesian leave-one-out cross-validation for model selection, *Comput. Brain. Behav.* **2**(1) (2019) 1–11.